ELSEVIER

Biophysical Chemistry 70 (1998) 41–56

Biophysical Chemistry

Probing the active site of adenosine deaminase by a pH responsive fluorescent competitive inhibitor

Valeria R. Caiolfa [a,1], David Gill [b], Abraham H. Parola [a,*]

[a] *Department of Chemistry, Ben Gurion University of The Negev, P.O. Box 653, Beer-Sheva 84 105, Israel*
[b] *Department of Physics, Ben Gurion University of The Negev, P.O. Box 653, Beer-Sheva 84 105, Israel*

Received 20 June 1997; revised 30 July 1997; accepted 21 August 1997

Abstract

The adenine analog erythro-9-(2-hydroxy-3-nonyl)adenine, EHNA, a tight reversible inhibitor ($K_I = 1.6 \times 10^{-9}$ M) of adenosine deaminase (EC 3.5.4.4) (ADase), was modified into the fluorescent etheno derivative ε-EHNA. The latter is a competitive inhibitor of adenosine deaminase [$K_I = (2.80 \pm 0.01)10^{-6}$ M], having the fluorescent properties of ε-adenines. Affinity to the active site, monitored by both steady-state and dynamic fluorescence polarization, was confirmed by competition experiments with 2′-deoxycoformycin, the substrate adenosine and EHNA. The ε-adenine moiety of ε-EHNA librates at the shallow active site of ADase. The low absorptivity of ε-EHNA required the measurement of fluorescence excitation spectra. Computer subtraction of fluorescence excitation spectrum of ADase from that of its equimolar complex with ε-EHNA revealed the corrected excitation spectrum of ε-EHNA at the active site of the enzyme. This spectrum mimics that of ε-EHNA at pH 5.5 in buffer solution, implying its protonation at the active site of the enzyme. These results are in agreement with the presence of acidic amino acids that are essential to the catalytic mechanism. © 1998 Elsevier Science B.V.

Keywords: Adenosine deaminase; Etheno-EHNA, Etheno analogues; Fluorescent competitive inhibitor; Protonation equilibrium; pH sensitive inhibitor of Adase

1. Introduction

Adenosine deaminase (adenosine aminohydrolase EC 3.5.4.4) (ADase) is an essential catabolic enzyme controlling the pool of adenosine and 2′-deoxyadenosine [1,2]. It affects cell differentiation and proliferation [3] and its reduced activity is associated with fatal immunodeficiency [4,5]. ADase is also an established malignancy marker, having anomalous activity in several cancers [6–11].

Abbreviations: ADase—adenosine deaminase; SS-ADase—small catalytic subunit of adenosine deaminase; ADCP—adenosine deaminase complexing protein; BSA—bovine serum albumin; PBS—sodium phosphate buffer saline; SDS-PAGE—sodium dodecyl sulfate polyacrilamide slab gel electrophoresis; Pentostatin—(2′-deoxycoformycin), [3-(2′-deoxy-β-D-erythro pento furanosyl)-3,6,7,8-tetrahydroimidazol (4,5-d) (1,3)diazepin-8-(R)-ol]; EHNA—erythro-9-(2-hydroxy-3-nonyl) adenine; ε-EHNA—1:N^6-etheno-[erythro-9-(2-hydroxy-3-nonyl)l adenine

* Corresponding author. Tel.: +972-7-6472454; fax: +972-7-6472943; e-mail: aparola@bgumail.bgu.ac.il
[1] Present address: Pharmacia and Upjohn, PPC-Oncology, V.le Pasteur 10, Nerviano (MI), Italy.

PII S0301-4622(97)00106-3

ADase has a variable quaternary structure. The small form (~ 45,000 Mr) of the human enzyme (SS-ADase) is a single polypeptide carrying less than 10% carbohydrates [12,13]. SS-ADase from various organs appears to be identical to that of erythrocytes [8,12]. The refined X-ray structures of murine ADA and its site-directed mutants are available at high resolution [14,15]. The large form ADase is a complex of SS-ADase with the complexing protein (ADCP) (2:1 molar ratio) [16]. ADCP (~ 210,000 Mr) is either soluble or membrane bound [8,17]. Quaternary structures can be interconverted in vitro [17] and hybrids of ADase subunits from different species (human, cow, sheep) are stable and active [9,18]. The biological role of ADase subunit polymorphism in various tissues is still unknown [8,18,19].

The problems related to this protein warranted the design and synthesis of active site directed fluorescent probes [20]. We have prepared a fluorescent adenine analog, ε-EHNA [2] (Chart 1),

Chart 1 Synthesis of ε-EHNA

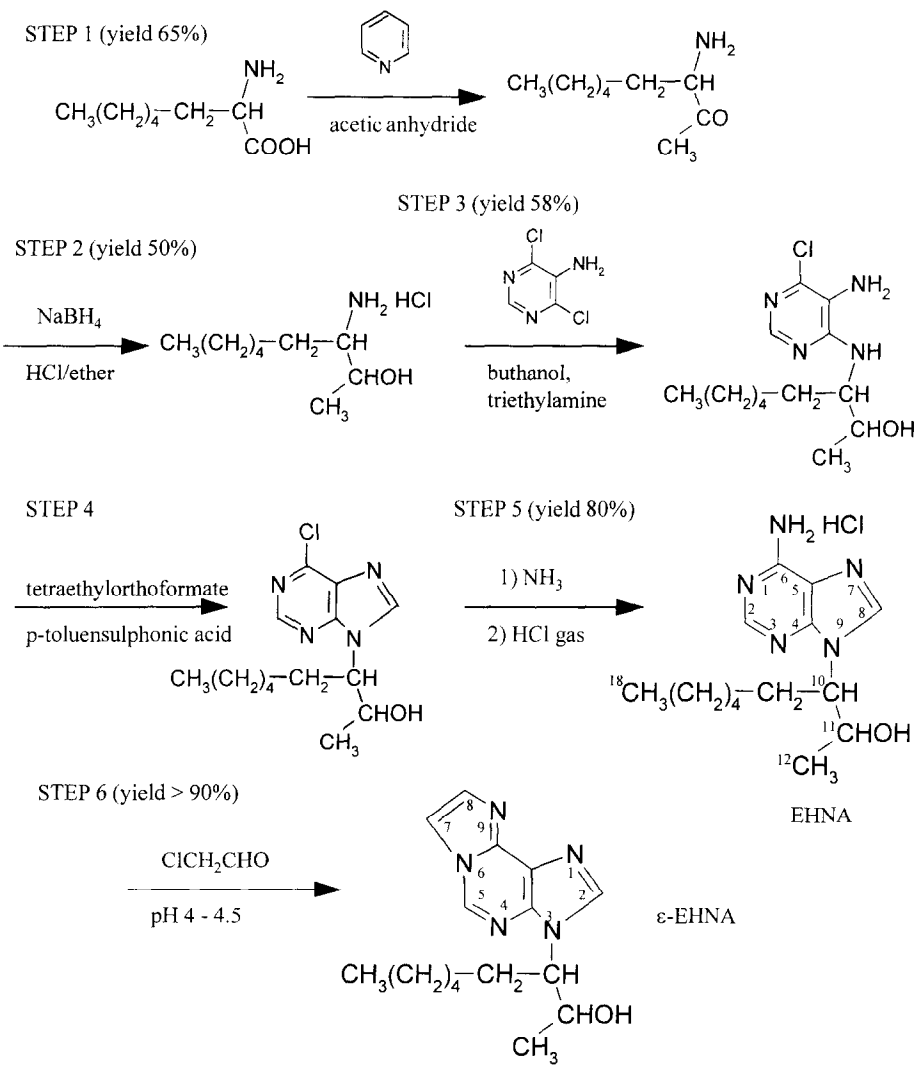

which is the etheno fluorescent modification of erythro-9-(2-hydroxy-3-nonyl)adenine, EHNA. The latter is a tightly binding specific inhibitor for ADase [21,22]. Fluorescent etheno–adenosine derivatives, initially introduced by Secrist III et al. [23], have been used to probe adenine-binding systems, be it nucleic acids or energy conserving substrates. Etheno–adenosine, obtained by reaction of aqueous chloroacetaldehyde with adenosine, is a modification of adenosine at the 6-NH_2 group (Chart 2).

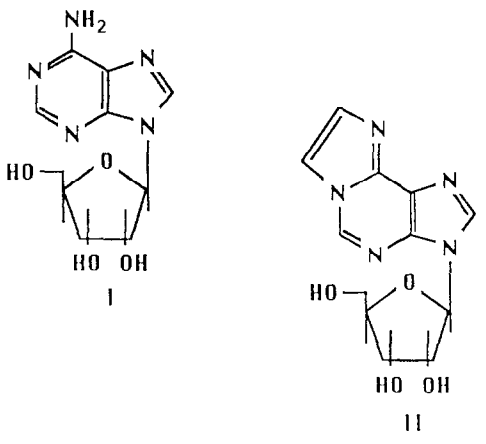

I adenosine
II ε-adenosine
III ε-EHNA

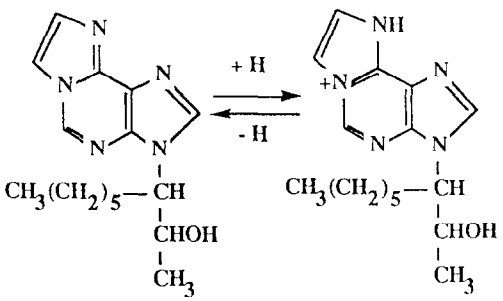

It fluoresces with a quantum yield close to 0.6 and a single lifetime of 23 ns [24,25]. The latter allows time resolved fluorescence and polarization studies of relatively high molecular weight proteins. Moreover, The pH dependence of its fluorescence excitation spectra may probe protonation equilibria (Chart 2).

EHNA, the immediate precursor of ε-EHNA is one of the tightest inhibitors of SS-ADase ($K_I = 1.6 \times 10^{-9}$ M). EHNA was classified neither as a ground state nor as a transition state inhibitor of SS-ADase; instead, it produces instantaneous inhibition followed by conformational changes [26,27]. It was suggested that incorrect binding of EHNA at the active site precluded its deamination.

We found that in ε-EHNA the fluorescence properties of etheno-analogs are retained. The fluorescent inhibitor is an additional tool, which can examine whether the binding site of ε-EHNA also is the active site of ADase. ε-EHNA is a competitive inhibitor of SS-ADase which binds to the active site of the enzyme with an inhibition constant ($K_I \sim 10^{-6}$ M), one order of magnitude better than adenosine. Its protonation upon binding to ADase, analogous to that reported with purine riboside [28] is indicative of its interaction with a strong acidic moiety at the active site.

[2] The abbreviation 'ε' was introduced by Leonard and co-workers and it stands for etheno.

2. Materials and methods

2.1. Materials

All reagents and solvents were analytical grade or purer. Adenosine deaminase (high purity grade, from calf intestine, approximately 200 units/mg protein) was purchased from Sigma Chemical as ammonium sulfate suspension or lyophilized powder. Total enzyme was estimated by SDS-PAGE [13] to be at least 90% pure 45,000 Mr subunits, while its activity was estimated to be 50% [27]. Ammonium sulfate was removed by dialysis against three changes of 10 volumes of PBS. BSA (fraction V, 96–99%), adenosine and ε-adenosine were purchased from Sigma Chemical Pentostatin (2′-deoxycoformycin) was obtained from Dr. Henry W. Dion, Director, Antibiotics and Microbial Development, Warner-Lambert, Parke-Davis (Michigan). Fluorescence spectroscopy grade glycerol was obtained from Merck. Thin layer chromatography was carried out on aluminum sheets of silica gel 60 F 254 pre-coated (5 × 7.2 cm, 0.2 mm thick) by Merck, unless indicated otherwise.

2.2. EHNA

The synthesis of ε-EHNA required first the preparation of EHNA. This was achieved following a combination of the procedures by Schaeffer and Schwender [21] and Sorolla [29] (Chart 1), with few modifications. Step #2: in the preparation of erythro 3-amino-2-nonanolhydrochloride, $NaBH_4$ was used as a reducing agent in absolute methanol and the temperature was maintained between −10 and −5°C. After extraction with chloroform and distillation under high vacuum, the product was precipitated from petroleum ether. Step #3: the ratio 5-amino-4,6 dichloro-pyrimidine-*n*-buthanol was reduced to 2 mmoles/ml. Step #5: EHNA was precipitated in ethanolic hydrogen chloride at 0°C. The solution was chilled overnight. Higher yield (1.5 fold) was achieved by additional bubbling of HCl gas, with the temperature kept below 20°C. Recrystallization was from methanol.

The m.p. of EHNA was that reported by Sorolla [29], 172–173°C, and TLC (CH_2Cl_2/CH_3OH, 90/10, v/v), showed only one spot with $R_f = 0.55$ observed in the iodine chamber and under UV light. We compared EHNA prepared by us with a sample cordially donated by Dr. H. Schaeffer of The Wellcome Research Laboratories, Burroughs Wellcome. A mixture 1 to 1 of the two compounds comigrated on TLC and melted at 173°C. ^{1}H NMR spectra were identical (see Chart 1 for atomic assignments) (DMSO-d_6, TMS internal reference): 0.78–1.80 ppm (m), 16 p, from C^{13} to C^{18} and C^{10}; ~ 3.5 ppm OH; 4.00 ppm (td), 3p, C^{12}; 4.38 ppm (qd), 1p, C^{11}; 8.44 ppm (s), 1p, C^2; 8.55 ppm (s), 1p, C^8; ~ 9 ppm NH_2. Furthermore, inhibition kinetics of adenosine deaminase lead to identical values of K_1 for both preparations of EHNA.

2.3. ε-EHNA

The reaction of EHNA with chloroacetaldehyde was according to Keeler and Campbell [30]. Chloroacetaldehyde in aqueous solution at pH 4.5 was obtained according to Secrist III et al. [23] from the hydrolysis in sulfuric acid of the corresponding dimethyl acetal (97%). The concentration of chloroacetaldehyde in solution was determined by a colorimetric assay with Schiff's reagent, [3] with a solution of paracetaldehyde as a calibration standard. ε-EHNA was prepared from 100 mg of EHNA dissolved in 2 ml of freshly prepared chloroacetaldehyde (1.57–1.70 M, pH 4.5). The mixture was stirred at room temperature in the dark for ~ 48 h, with pH kept between 4.0–4.5 by addition of NaOH 0.1 N. The reaction was monitored by TLC and by UV spectroscopy. Absorbance was recorded on 10 μl of the reaction mixture diluted 100-fold in 63 mM sodium phosphate buffer at pH 7.5. The reaction was stopped when the ratio of the absorbance at 266 nm to that at 276

[3] Schiff's reagent (fuchsine aldehyde reagent) was prepared according to Vogel, Qualitative Organic Chemistry, 3rd edn., p. 331, Longman, 1972.

nm became constant. After evaporation of excess chloroacetaldehyde under vacuum (at ~ 50°C), the crude mixture was washed with methanol and evaporated again. Finally, the residue was slurred in methanol and chilled at 4°C overnight. After solvent evaporation, ε-EHNA was recovered and purified either by recrystallization from mixed solvents or by preparative cellulose TLC. In the first case, the crude product was dissolved in a minimal amount of ethanol and diethyl ether was added until the solution turned cloudy. Subsequently, it was chilled at 4°C for 24 h to complete the precipitation. Recrystallization was repeated twice with 90% recovery of the product. In the second case, crude ε-EHNA (50 mg) was dissolved in a minimum of ethanol and loaded on a 20 × 20 cm plate of microcrystalline cellulose (1.3 mm thickness). Chromatography was carried out in the dark, at room temperature in isopropanol: NH_4OH (conc): H_2O (70:10:20, v/v). The fluorescent band was recognized under UV light. ε-EHNA was extracted with distilled water (acidified at pH 4.5) and the cellulose separated in an Eppendorf centrifuge (9980 × *g*). The extract was evaporated at 50°C under vacuum. About 30 mg (60%) of white product were recovered after drying under high vacuum for 24 h at room temperature.

The successful introduction of the etheno bridge on EHNA was verified by fluorescence and proton magnetic resonance. ^{1}H NMR (DMSO-d_6, TMS internal reference) revealed two doublets at 7.81 ppm and 8.25 ppm, originating in hydrogens at C^7 and C^8. The singlets at 8.53 ppm and 9.44 ppm indicating the hydrogens at C^5 and C^2 respectively were also present. (see Chart 1 for atomic assignments). The assignments on the heterocyclic moiety were based on published studies [24,31,32] of deuterium labelling in either $ClCD_2CHO$ or [8-D]adenosine. The relative chemical shifts and coupling constants were found consistent throughout a series of adenosine nucleotides and the order of the chemical shifts was shown to remain the same for 9-alkyl-substituted bases in that series. Purified ε-EHNA showed only one blue fluorescent spot on TLC without fluorescent indicator, (CH_2Cl_2/CH_3OH, 90/10, v/v), $R_f = 0.50$ in an iodine chamber and by UV light. On TLC with fluorescent indicator, (CH_2Cl_2/CH_3OH 90/10, v/v), still only one spot was detectable.

2.4. Protein assay

Protein was assayed according to the procedure of Sedmak and Grossberg [33] using aqueous solutions of BSA as the standards.

2.5. Adenosine deaminase activity

The enzymatic activity was determined by spectrophotometric assay at 265 nm [9,12,13]. Enzyme kinetics were run at 24 ± 1°C. The concentration of SS-ADase was calculated assuming $M_r = 45{,}000$. SS-ADase was incubated 5 min with either ε-EHNA, EHNA or ε-adenosine prior to addition of adenosine. In the spectrophotometric method, the concentration of adenosine was varied from 1.0×10^{-5} to 166×10^{-5} M. Curves of decreasing absorbance at 265 nm were recorded as long as they showed a constant slope, for intervals of time ranging from 30 s to 3 min.

2.6. Photobleaching

Photobleaching of non-peptide fluorescent impurity ($\lambda_{ex}^{max} = 350$ nm; $\lambda_{em}^{max} = 420$ nm) was carried out at 355 nm (the third harmonic of a Nd: YAG laser) way above wavelengths absorbed by protein tryptophans, according to the procedure already described by us [34].

2.7. Absorption and fluorescence spectroscopy

The spectra were recorded with a Spectronic 2000, Bausch and Lomb double beam spectrophotometer at room temperature.

Fluorescence emission spectra were recorded at room temperature on a PC-interfaced Perkin-Elmer MPF44 spectrofluorometer. Slits were set at 4 nm for both excitation and emission monochromators.

Corrected excitation spectra were recorded on an SLM 4800 spectrofluorometer with a depolarizer at the exit of the excitation monochromator, at emission wavelength of 400 nm. The depolarizer averaged the polarized components originating in the monochromator grating. All measurements with depolarized excitation included an emission polarizer at 34° to the vertical. A concentrated solution of Rhodamine B in propylene glycol was used as reference.

2.8. Limiting anisotropy

The limiting anisotropy of a solution of ε-EHNA in 50% glycerol in sodium phosphate buffer, pH 7.5 (absorbance at 315 nm < 0.1, [35]) was determined on the SLM 4800 equipped with Glan polarizers [*T*-configuration, excitation at 315 nm, slits set at 4 nm for both excitation and emission, Kodak Wratten 400 nm sharp cut-off (Turner, C.S. 2A) emission filter, depolarizer at the exit of the excitation monochromator prior to the Glan excitation polarizer]. The sample chamber was thermostated and kept dry under nitrogen flow. The anisotropy of the sample, in a 3 ml quartz cuvette, was measured as a function of temperature, the latter being checked inside the cuvette by a tele-thermometer (± 1°C). Average anisotropy values of at least three independent measurements at each temperature were obtained.

2.9. Polarized excitation spectrum of ε-EHNA

The polarized excitation spectrum of ε-EHNA at 4°C was obtained with the Perkin-Elmer MPF-44 spectrofluorometer as described for the relative fluorescence emission studies. ε-EHNA was in 50% propylene glycol as described in the limiting anisotropy studies. The emission was set at 400 nm, excitation spectra were recorded at the four relative orientations of the polarizers and elaborated by computer to obtain the polarization as a function of the wavelength.

2.10. Fluorescence lifetime

Lifetimes were measured on the SLM 4800 phase-modulation spectrofluorometer, equipped with a depolarizer at the exit of the excitation monochromator, followed by a Glan excitation polarizer set vertically and an emission polarizer set at a 55°. With excitation at 315 nm, fluorescence emission was passed through a Kodak Wratten sharp cut-off filter at 400 nm (Turner, C.S. 2A). The phase reference was a zero-lifetime (scattering) solution or the fluorescence standard PPO in absolute ethanol (1.61 ns) [36]. At least five measurements of phase and modulation were accumulated at 6, 18 and 30 MHz in accumulation time windows of 25 s, and converted into τ_{phase} and τ_{mod} by SLM lifetime software. Heterogeneity analysis of τ_{phase} and τ_{mod} data was carried out by least-squares analysis program ISSC6-87, assuming phase and modulation frequency-independent measurement errors, $\sigma_{phase} = 0.2$ and $\sigma_{modulation}$ 0.004, respectively [37].

2.11. Steady-state polarization

Polarization of ε-EHNA as a function of SS-ADase concentration, at 22 ± 1°C, was measured as in Refs. [38–40]: (1) Perkin-Elmer MPF-44 equipped with dichroic excitation and emission polarizers and a depolarizer, placed at the entrance to the emission monochromator, $\lambda_{ex} = 315/\lambda_{em} = 400$ nm; excitation and emission slits were 6 and 20 nm respectively; (2) SLM 4800, *T*-configuration, equipped with Glan polarizers and a depolarizer at the entrance to the emission monochromator, at $\lambda_{ex} = 315$ nm, with either 350 nm or 400 nm Kodak Wratten sharp cut-off filters (e.g., Turner, C.S. 2A) in front of the emission photomultipliers. Samples were prepared from freshly bleached SS-ADase in 63 mM sodium phosphate buffer, pH 7.5. The concentration of ε-EHNA was kept constant in all samples (5×10^{-6} M, in phosphate buffer, pH 7.5) while SS-ADase concentration was varied from 3.33×10^{-7} M to 9.45×10^{-6} M. The concentration of SS-ADase was determined from the blanks

(equal concentration of enzyme in the absence of ε-EHNA) by the spectrophotometric activity assay, assuming a molecular weight of 45,000.

2.12. Dynamic polarization

Dynamic polarization of ε-EHNA as a function of SS-ADase:ε-EHNA molar ratio was measured on an SLM 4800 at $\lambda_{ex} = 315$ nm, at modulation frequencies of 6 and 30 MHz and T-configuration (in accumulation time windows of 25 s, with a depolarizer at the exit of the excitation monochromator followed by an excitation polarizer: Kodak Wratten sharp 400 nm cut-off filter in front of the emission photomultipliers). Measurements were recorded either by rotating the excitation polarizer from 0° to 90° with polarizer in channel A at 0° and polarizer in channel B at 90° or, according to Lakowicz et al. [41], by rotating channel B polarizer from 0° to 90° with polarizers in channel A and excitation both at 0°.

3. Results

3.1. Spectroscopy of ε-EHNA

The spectroscopic properties of ε-EHNA are similar to those of ε-adenosine with respect to low absorptivity (Fig. 1) [23,42], long fluorescence lifetime (Table 1) [24], the pH dependence of both absorbance (Fig. 1) [42] and fluorescence intensity (Fig. 2) or lifetime (Table 1) [23,24,43] and the independence of fluorescence emission maximum on solvent polarity (data not shown). The differences are: (1) the molar absorptivity of the strongest band (276 nm) is only 3570 M^{-1} cm^{-1}, compared to 8120 M^{-1} cm^{-1} (260 nm) of EHNA. A similar change in the absorptivity was observed in ε-adenosine: it declined to 6000 M^{-1} cm^{-1} (275 nm at pH 7.0) from that of adenosine, 14,000 M^{-1} cm^{-1} (260 nm) [24,42]. Thus, ε-EHNA has only 44% of the absorptivity of ε-adenosine; (2) Fluorescence lifetime at pH 7.5 is 27.12 ± 0.18 ns, longer than in other ε-adenines; (3) At pH = 2.3 two (rather than one) relatively short lifetimes appear (Table 1).

Fig. 1 shows the absorption spectra of ε-EHNA as a function of pH. The acidity constant of ε-EHNA, $pK_a^{\varepsilon\text{-EHNA}}$, was derived from a plot of absorptivity vs. pH (Fig. 1b). $pK_a^{\varepsilon\text{-EHNA}}$ was calculated at four different wavelengths the average value of 4.03 ± 0.19 was obtained. A plot of the peak fluorescence intensity versus pH is shown in Fig. 2. A non-linear least square analysis yielded pK_a of fluorescence of 4.11 ± 0.12 ($r^2 = 0.98$), as did a lifetime titration (Table 1). This pK_a is consistent with that obtained from the UV–pH titration data [43]. A drop in fluorescence intensity beginning at pH 8.0 was observed (data not shown), presumably caused by hydrolytic ring opening of the ε-adenine moiety to a bi-imidazole [23,43].

Corrected fluorescence excitation spectra of ε-EHNA as a function of pH are shown in Fig. 3. An isosbestic point in the range of pH 4.4–7.5 is revealed at about 290 nm. At pH 10.0, the observed drop in fluorescence excitation intensity, as well as the deviation from the isosbestic point is presumably caused by the hydrolytic ring opening of the ε-adenine moiety [24]. UV absorbance of ε-EHNA in phosphate buffer at pH 7.5 (Fig. 1) differs from the fluorescence excitation spectrum (Fig. 3), the short-wavelength half of which is attenuated. The short wavelength half, peaking at 276 nm, consists of absorbance by protonated ε-EHNA, as well as by the unprotonated species (Fig. 1). Both protonated and unprotonated species absorb but only the unprotonated one fluoresceses. The curve obtained at pH 3.5, i.e., at high proton concentration, triggered our study on the role that ground and excited state protonation play in the photophysics of ε-adenines. It led to our suggestion of a unique $n \rightarrow \pi^*$ fluorescence transition. This suggestion accounts for the unusually long lifetime of these compounds, resolving a three decade debate in the literature [25].

Perrin plot of ε-EHNA in glycerol [4] (50% in phosphate buffer, pH 7.5) was linear from −40°C to +20°C,

[4] Viscosity of glycerol at different temperatures was obtained from the International Critical Tables Handbook of Chemistry and Physics and Perry's Chemical Engineers Handbook, applying the Guzman–Andevage equation: $\eta = A \exp(B/T)$, where A and B are empirical constants.

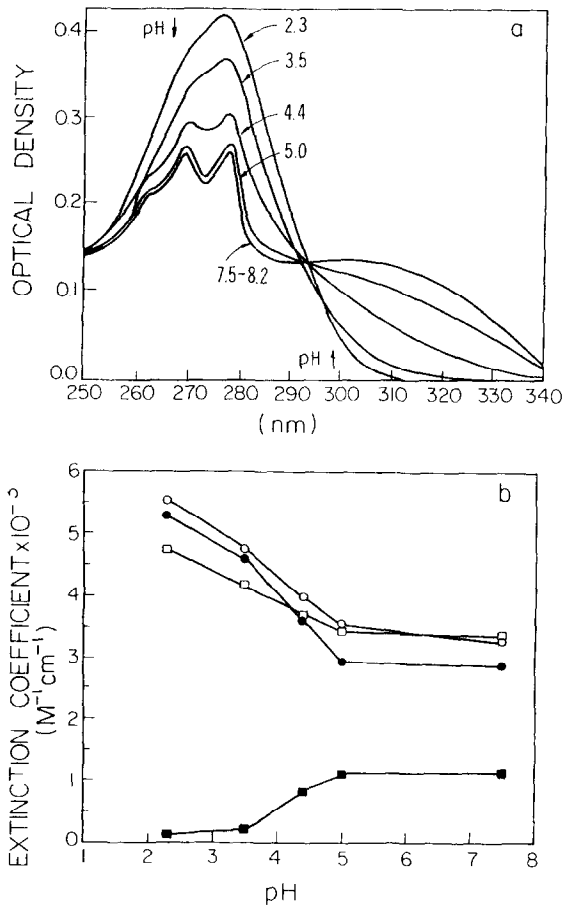

Fig. 1. Dependence of the UV spectra of ε-EHNA on pH in buffered solutions at [ε-EHNA] = 0.1 mM, at room temperature: (a) change of the UV spectrum resulting from the increase of pH from 2.3 to 8.2; (b) Evaluation of the spectra shown in (a) by plotting the absorptivity vs. pH at (○) 276 nm, (□) 266 nm, (●) 273 nm and (■) 310 nm.

Table 1
Fluorescence lifetime of ε-EHNA as a function of pH[a]

pH	τ (ns)	α[b]	χR^{2}[c]
9.0	27.13±0.20	1	1.14
8.4	27.24±0.17	1	1.13
7.5	27.12±0.18	1	1.20
7.0	27.02±0.15	1	1.27
6.4	26.74±0.22	1	2.06
4.6	24.36±0.32	1	5.55
3.5	5.84±0.12	1	1.42
2.3	2.19±0.90 (τ_1)	0.27±0.20	11.52
	10.51±1.62 (τ_2)	0.73±0.20	

[a]The fluorescence lifetimes (τ) are calculated values from heterogeneity analysis on τ_{phase} and τ_{mod} data at 6, 18 and 30 MHz, assuming for phase and modulation frequency independent measurement errors [37].
[b]α is the fractional contribution of each lifetime component. It is obviously equal to unity for a monoexponential decay.
[c]χR^2 is the residual chi-square which indicates the goodness of the fit between experimental and calculated data [37].

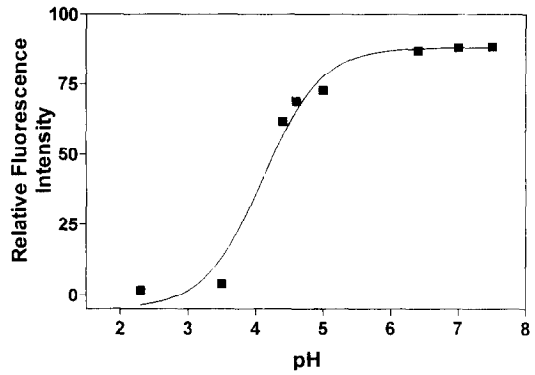

Fig. 2. pH profile of the relative fluorescence emission maxima (at 400 nm) of ε-EHNA. Excitation was at 315 nm, at room temperature. Buffered solutions of ε-EHNA were 0.1 mM. The average error was $\pm$ 1%. The line represents the non-linear least square fitting of the data ($r^2 = 0.98$).

indicating a single rotational correlation time. The limiting anisotropy, obtained by extrapolating the curve to $T/\eta = 0$, was $r_0 = 0.23$ and the polarization as a function of the wavelength had features similar to those of ε-adenosine i.e., monotonic increase of P with increasing wavelength (data not shown).

3.2. Enzyme kinetics

SS-ADase initial rate kinetics were studied in the presence of EHNA, ε-EHNA and ε-adenosine (Fig. 4 and Table 2). K_m of adenosine, 1.67×10^{-5} M $\pm$ 0.12×10^{-5} SE, resembled the literature value, 2.5×10^{-5} M [21]. The inhibition constant of the newly synthesized EHNA was a good test of its biochemical potency, prior to the synthesis of its derivative ε-EHNA. A sample of EHNA was kindly donated by The Wellcome Research Lab., Burroughs Wellcome, yielded $K_I = 1.46 \pm 0.82 \times 10^{-9}$ M in our hands. Our preparation of EHNA gave a $K_I = 1.32 \pm 0.03 \times 10^{-9}$ M. Both values are in good agreement with the published one ($K_I = 1.6 \times 10^{-9}$ M) [44]. Non-linear least square analysis of initial rate kinetics of SS-ADA in the presence of ε-EHNA and ε-adenosine (Fig. 4 and Table 2) yielded the same V_{max} values which are consistent with a competitive

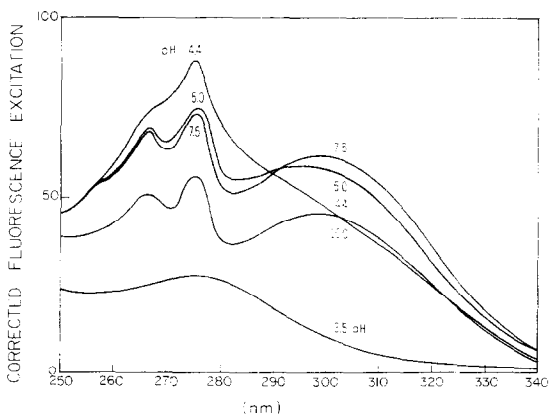

Fig. 3. Corrected fluorescence excitation spectra of ε-EHNA as a function of pH. Fluorescence emission at 400 nm, 22 $\pm$ 1°C, [ε-EHNA] = 0.1 mM. Fluorescence excitation differs from UV absorption in that the unprotonated form (e.g., pH 7.5) contributes more to fluorescence than the protonated one.

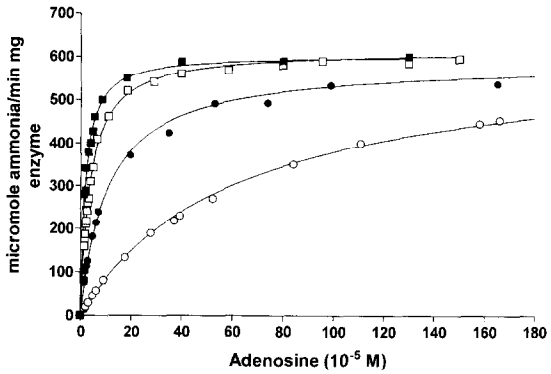

Fig. 4. Initial rate kinetics of SS-ADase at room temperature (25°C) in phosphate buffer 63 mM, at pH 7.5. (■) [SS-ADase] = 1 nM; (□) [SS-ADase] = 1 nM, [ε-adenosine] = 27 μM; (●) [SS-ADase] = 1 nM, [ε-EHNA] = 15 μM; (○) [SS-ADase] = 2 nM, [EHNA] = 48.5 nM. Substrate concentration, [adenosine] = $1-166 \times 10^{-5}$ M.

mechanism of inhibition. Accordingly, the calculated inhibition constants are: $K_I^{\varepsilon\text{-EHNA}} = (2.80 \pm 0.01) \times 10^{-6}$ M and $K_I^{\varepsilon\text{-adenosine}} = (2.22 \pm 0.05) \times 10^{-5}$ M (Table 2). These values are the mean of at least three experiments.

3.3. Fluorescence polarization as a monitor of binding

SS-ADase had a typical, non-peptidic, fluorescence [34], which coincided and interfered with the fluorescence emission of ε-EHNA. Accordingly, we photobleached the enzyme, resulting in a sevenfold decrease of the nonpeptidic fluorescence with negligible loss of enzymatic activity. The enzymatic and spectroscopic integrity of the photobleached protein was fully proved [34].

Etheno derivatives were insensitive to the polarity of the medium and, indeed, binding to SS-ADase did not shift the fluorescence emission maximum of ε-EHNA.

The binding of ε-EHNA to non-photobleached as well as photobleached SS-ADase raised the steady-state polarization. With the photobleached enzyme, polarization reached a plateau for a [SS-ADase]:[ε-EHNA] molar ratio smaller than 1 to 1 and the maximum value of polarization was 0.028 ± 0.002 (Fig. 5a, Table 3). With unbleached enzyme, at the same range of concentrations, polarization did not reach a plateau value up to a

Table 2
Initial rate kinetics of SS-ADA[a]

	$V_{max} \pm$ SE[b]	$K_{app} \pm$ SE (10^{-5} M)	$K_I \pm$ SE (M)[c]	r^{2d}	(n)
Adenosine	588 ± 11	1.67 ± 0.12		0.98	(21)
ε-Adenosine	603 ± 4	3.72 ± 0.10	$2.22\ 10^{-5} \pm 0.05$	0.99	(20)
ε-EHNA	587 ± 5	10.57 ± 0.30	$2.80\ 10^{-6} \pm 0.01$	0.99	(22)
EHNA	601 ± 6	60.43 ± 1.47	$1.32\ 10^{-9} \pm 0.03$	0.99	(22)

[a]Non-linear least square fitting was carried out according to the following equation: $v = (V_{max}\ [Sub])/(K_{app} + [Sub])$; where v is the reaction rate, [Sub] is the concentration of adenosine.
[b]V_{max} = micromoles ammonia/min × mg enzyme.
[c]$K_{app} = K_m\ (1 + [I]/[K_I])$, where $[I]$ is the concentration of the inhibitor, K_m is the Michaelis–Menten constant of adenosine and K_I is the inhibition constant for a competitive inhibitor.
[d]r^2 = correlation coefficient with n = number of data points.

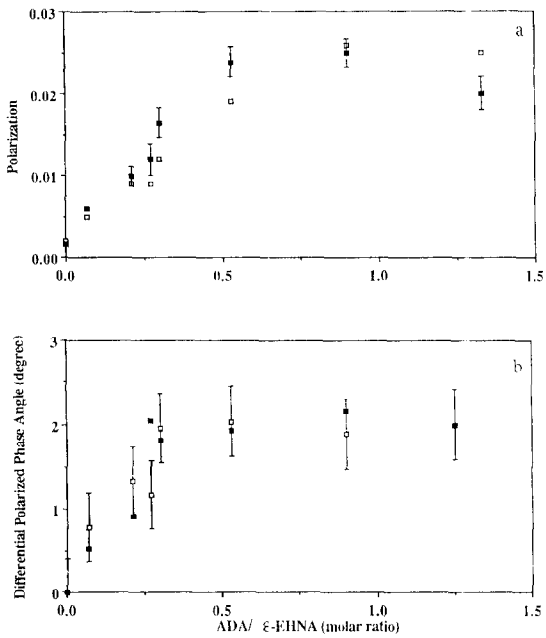

Fig. 5. Binding of ε-EHNA to SS-ADase followed by (a) steady state polarization and (b) differential polarized phase angle at 6 MHz, at 22 ± 1°C, in 63 mM sodium phosphate buffer, pH 7.5. The concentration of ε-EHNA was maintained constant, 1 μM. Empty squares are fluorescence polarization measurements in the T-shape geometry and the filled ones are L-shaped geometry.

[SS-ADase]:[ε-EHNA] ratio of 13. In these steady state fluorescence polarization measurements, each polarized intensity was corrected by subtracting the respective value of a blank sample. Nevertheless, artefact fluorescence polarization values could be obtained when the contribution of the unbleached enzyme exceeded 10%. Accordingly, we adopted laser photobleaching as a routine for the rest of this study [34].

Table 3
Lifetimes and polarization of free and bound ε-EHNA

ε-EHNA		Lifetime distribution[a] at 25°C (ns)	Lifetime[b] weighted average (ns)	P[c] at 25 °C	r_0[d]	$\Delta\Phi$[e] at 25°C (degrees)
Free in buffer, pH 7.5		27.12 ± 0.18		0		
Free in 50% glycerol (in buffer, pH 7.5)		23.20 ± 0.42		0.034[f] (±0.005)	0.23	
Bound to SS-ADase 1:1 complex	τ_1	24.60 ± 1.06	20.26	0.028 (±0.002)		2.0 ± 0.5
(in buffer, pH 7.5)	α_1	0.80 ± 0.02				
	τ_2	2.90 ± 0.42				
	α_2	0.20 ± 0.02				
Bound to SS-ADase 1:1 complex	τ_1	22.88 ± 3.63	12.60	0.061 (±0.001)	0.11	
in 50% glycerol (in buffer, pH 7.5)	α_1	0.49 ± 0.05				
	τ_2	2.79 ± 0.39				
	α_2	0.51 ± 0.05				

[a] Calculated values of lifetime by heterogeneity analysis.
[b] τ mean$^{(\text{weighted})} = \Sigma\alpha_i\ \tau_i/\Sigma\alpha_i$ (i = component of the decay; α = fractional contribution).
[c] Steady-state polarization at 315 nm excitation: $P = (I_{VV} - G \times I_{VH})/(I_{VV} + G \times I_{VH})$. $G = I_{HV}/I_{HH}$.
[d] Limiting anisotropy, according to Perrin equation (see text).
[e] Differential polarized phase angle at 6 MHz (see text and Fig. 5b).
[f] At 20°C.

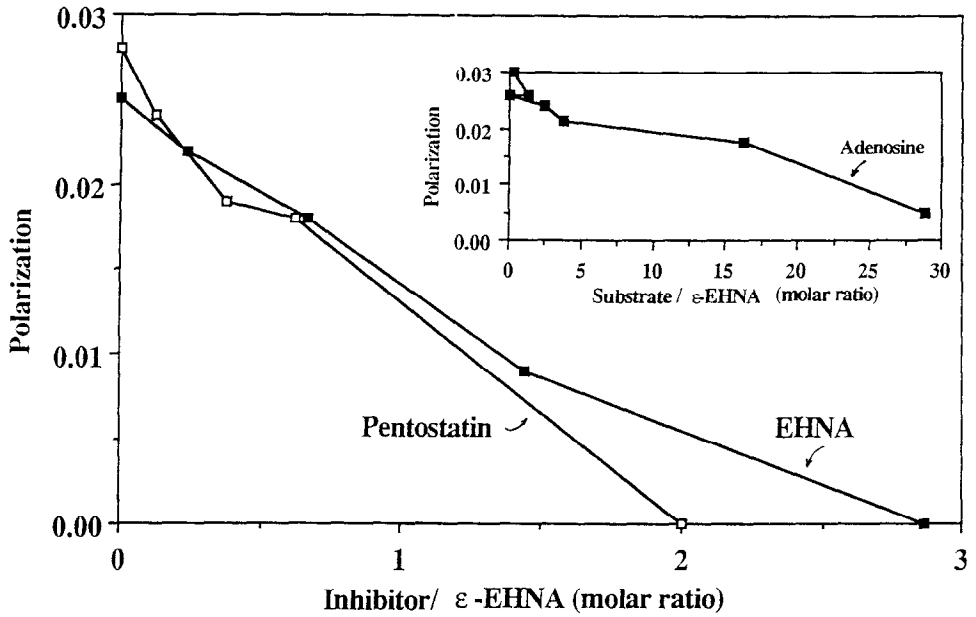

Fig. 6. Fluorescence polarization of the SS-ADase: ε-EHNA complex (molar ratio 1:1, 1 μM) as a function of increasing amounts of Pentostatin (2′-deoxycoformycin), EHNA and (insert) the substrate adenosine. λ_{ex} = 315 nm, λ_{em} = 407 nm, 22 ± 1°C.

The following lifetimes of ε-EHNA bound to SS-ADase were derived from the heterogeneity analysis: $\tau_1 = 24.60 \pm 1.06$ ns and $\tau_2 = 2.90 \pm 0.42$ ns with fractional contributions of 0.80 and 0.20 (±0.02) respectively (Table 3). The difference in average lifetime between free and bound ε-EHNA is too small to account for the relatively large change in polarization. The polarization did not change upon 30-fold dilution of the sample of SS-ADase: ε-EHNA (1:1 molar ratio), indicating the absence of polarization due to scattering. Obviously dissociated ε-EHNA with P approaching zero does not affect the overall P value. In the presence of BSA, neither increase of polarization nor change of ε-EHNA lifetime was observed up to a 25 to 1 [BSA]:[ε-EHNA] molar ratio. Furthermore, a similar saturation curve was obtained by measuring the differential polarized phase angle at 6 MHz (Fig. 5b); at such frequency, the long lifetime contribution of ε-EHNA is preferentially monitored. We thus concluded that the observed increase in fluorescence polarization, though small, indicates reduced rotational freedom caused by binding of ε-EHNA to the enzyme; it is not an artifact caused by either increased scattering or background fluorescence of the enzyme.

3.4. Binding to and protonation at the active site

Specificity of binding was confirmed by competition with Pentostatin ($K_I = \sim 10^{-12}$ M, [44], EHNA ($K_I = 1.46 \times 10^{-9}$ M) and the substrate adenosine (Fig. 6). Complete or almost complete loss of polarization occurred as the ratio of inhibitor or substrate to ε-EHNA increased. The observed 2:1 [Pentostatin]:[ε-EHNA] required to displace the ε-EHNA may be traced to impurity in the protein or the label.

We attempted to correlate our steady-state and dynamic fluorescence polarization data so as to extract the rotational correlation time of ε-EHNA. We applied the Perrin equation ($r_0/r = 1 + \tau/\phi$) and drew a Perrin plot of the 1:1 SS-ADase:ε-EHNA complex (in 50% glycerol in 63 mM sodium phosphate buffer, pH = 7.5) (data not shown) [45]. In Table 3, the results of free and SS-ADase-bound ε-EHNA in buffer and in 50% glycerol are compared. Two-lifetime distributions are observed for the complex in buffer, differing from those in glycerol. Then, the Perrin plot of the complex in 50% glycerol showed at least two slopes, indicating two or

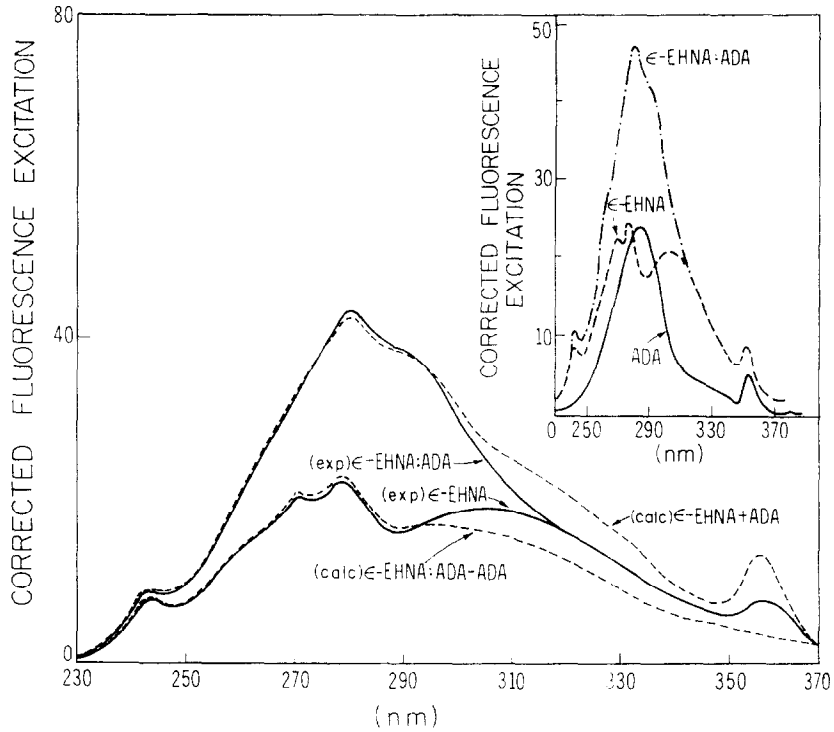

Fig. 7. Inset: corrected fluorescence excitation spectra, in phosphate buffer at pH 7.5, at $\lambda_{em} = 400$ nm and at room temperature, of: (- · -) SS-ADA; ε-EHNA 1 to 1 complex, 1 μM; (- - -) ε-EHNA, 1 μM; (————) SS-ADase, 1 μM ($M_r = 45{,}000$; laser photobleached). Figure: Full lines—expanded view of (- · -) and (- - -) of insert. Lower dashed curve: computer subtraction of (—) from (- · -) of insert. This curve is the spectrum of ε-EHNA at the active site of SSADase. The absence of the Raman line at 360 nm validates the subtraction procedure. This curve mimics that of ε-EHNA in buffer at pH 5.5. Upper dashed curve: computer addition (from insert) of ε-EHNA, in buffer at pH 7.5 (- - -) and SS-ADase, in buffer at pH 7.5 (————). This reference spectrum represents a non-interacting 1 to 1 mixture. All spectra were free of inner filter effect (absorbance < 0.2).

Table 4
pH dependence of fluorescence characteristics of ε-EHNA

peak ratio	Relative fluorescence[a] 276/300 nm ratio	Corrected excitation[b]
ε-EHNA in buffer[c]		
9.0	0.84	-
8.0	0.92	-
7.5	1.00	1.17
5.5	0.82	1.34
4.4	0.69	1.85
3.5	0.05	-
2.3	0.02	-
ε-EHNA bound to SS-ADase		
	0.82	1.35

[a] Since no shift in the maximum of fluorescence emission was observed as a function of pH, fluorescence intensity changes can be represented as the ratio between the peak height at a given pH and that at pH 7.5, at a constant concentration of ε-EHNA.
[b] This is the ratio of the peak height at the two representative wavelengths.
[c] The data point related to pH 10 (Fig. 3) was not included because of the hydrolytic ring opening of the ε-adenine moiety (see text).

more rotational correlation times (ϕ). Hence, models assuming a single lifetime and a single rotational correlation time are not applicable to our system.

The corrected fluorescence excitation spectra of SS-ADase:ε-EHNA equimolar complex (Fig. 7 inset) can be interpreted as the sum of two comparable contributions from the label and from the enzyme, respectively. Subtraction of the enzyme contribution from the corrected excitation spectrum of SS-ADase:ε-EHNA equimolar complex (Fig. 7) might be interpreted as the spectrum of ε-EHNA in the active site of SS-ADase. This corrected spectrum is similar to the one obtained in a buffer at pH = 5.5. Quantitative indicators for comparing the spectra are given in Table 4 as relative fluorescence emission peak ratios at 400 nm and corrected fluorescence excitation ratios 276/300 nm. The corresponding values for ε-EHNA bound to SS-Adase are also included. This analysis is supported by the fact that the major spectral differences between bound and free ε-EHNA are detectable in that region where the spectral contribution of the enzyme is much reduced (i.e., above 315 nm). Accordingly, while spectral contribution due to enzyme conformational changes associated with complex formation is not expected, it might result in a marginal effect, if at all.

4. Discussion

The present study suggests the binding of ε-EHNA to ADase at the active site, where the ε-adenine moiety librates freely and may undergo protonation.

The introduction of the etheno ring to adenosine or to EHNA does not prevent their binding to SS-ADase and, in fact, both etheno derivatives are competitive inhibitors of the enzyme (Fig. 4); the inhibition constant of ε-adenosine is very close to the K_m of adenosine. Inhibition by ε-EHNA is an order of magnitude stronger than by ε-adenosine and 3′-*O*-dansyladenosine [20] (Fig. 4, Table 2). Undoubtedly, it is the hydrophobic moiety in ε-EHNA which enhances its binding to SS-ADase (relative to ε-adenosine), since the two compounds are otherwise equal.

In ε-EHNA, fluorescence can be used to monitor binding competition with the native substrate, adenosine, or with 2′-deoxycoformycin which is a classical transition-state inhibitor, definitely binding to the active site. Utilizing steady state fluorescence polarization, which indicates immobilization of ε-EHNA upon binding to SS-ADase, we observed saturation binding (Fig. 5). Differential polarized phase fluorometry (Fig. 5b) at 6 MHz yielded a binding curve similar to that of steady-state polarization (Fig. 5a). The specific binding of ε-EHNA to the active site of SS-ADase is indicated by the complete loss of fluorescence polarization after the addition of stronger inhibitors such as Pentostatin (2′-deoxycoformycin) or by the almost complete loss in the presence of 30-fold excess of the native substrate, adenosine (Fig. 6). Since EHNA displaced ε-EHNA as did Pentostatin, it presumably competed for the same site. Furthermore, as detailed below, ε-EHNA might undergo protonation upon binding to the enzyme. Such a protonation process is expected at the active site of ADase, being the first step of substrate catalysis [46].

Perrin plots in 50% glycerol showed at least two slopes, indicating at least two rotational correlation times (ϕ). We suggest a relatively fast motion of the label inside a slowly tumbling protein (Table 3). This may be the cause of the relatively low steady-state polarization and the lowered extrapolated limiting anisotropy ($r_0^{complex} = 0.11$ vs. $r_0^{free} = 0.23$, Table 3). The ε-adenine moiety may librate within the shallow active site of ADase, with even more freedom than it does in 50% buffered glycerol. Indirect kinetic data led Leonard [47] to suggest long ago a shallow active site in ADase which is presently confirmed. The nonyl chain docks ε-EHNA near the active site [27], allowing the ε-adenine moiety to librate.

The pH dependence of the fluorescence of ε-EHNA may enable the study of protonation equilibrium. This application rests on two assumptions: (1) since both absorption and fluorescence are pH dependent, each in its own way, either one of them can be calibrated to measure apparent pH. (2) If pK_a of enzyme bound ε-EHNA is close to that in buffer solution, then the spectra can be used to measure pH. This presumed constancy of pK_a is expected from an etheno–adenine moiety which interacts weakly with the binding site, as indicated by the lowered inhibition constant (relative to EHNA, Table 2) and polarization value ($P = 0.028 \pm 0.002$).

Our results indicate an apparent pH of 5.2–5.5 at the active site of SS-ADase (Table 4) although that of the buffered bulk is 7.5. They may support the calculations of Warshel [48] who suggested that enzymes can be viewed as 'super solvents' that stabilize (solvate) ionic transition states [5] more effectively than do aqueous solutions. This solvation is attained by enzyme dipoles folding in a cryptate-like pattern around the developing charged species. The relatively low 'apparent pH' implies a strongly acidic moiety at the active site. The ratio of protonated to non-protonated ε-EHNA at this apparent pH 5.5 as read in the active site, should be 1 to 25, while at the buffered bulk pH of 7.5 this ratio is about 1 to 3000. According to NMR studies, the interaction of SS-ADase with purine riboside was suggested to consist of protonation and rehybridization at the C-6 carbon, resulting in a tetrahedral transition state analog [28]. This rehybridization is not feasible for ε-EHNA because of the etheno moiety. Still, the initial protonation reported by ε-EHNA implies the proximity to a relatively acidic groups [49]. Site-directed mutations recently revealed that the substitution of acidic amino acids in the active site of human SS-ADA, such as Glu217, dramatically reduces the deaminating activity of the enzyme [50].

In ε-EHNA, three orders of magnitude are lost relative to the overall inhibitory power of EHNA (Table 2). Frieden et al. [27] observed that the inhibition by EHNA is a two step process: a rapid initial binding step with an inhibition constant of 2×10^{-7} M followed by a second step with a rate constant in the forward direction 120 times greater than that in the reverse reaction. The overall inhibition constant is $K_1 = 1.6 \times 10^{-9}$ M. They proposed an initial step (classical competitive inhibition) of incorrect binding of EHNA to the active site followed by a rearrangement of either the enzyme or the inhibitor, resulting in a complex from which EHNA can escape only slowly. Comparing the inhibition constant of the initial step with that of purine riboside ($\sim 1 \times 10^{-6}$ M) and adenosine itself ($K_m = 2 \times 10^{-5}$ M), Frieden et al. [27] pointed to the crucial role of the nonyl chain in the binding of EHNA to SS-ADase. In the present study however, the reduced inhibition constant of ε-EHNA (even with respect to the initial binding of EHNA, $K_1 = 2 \times 10^{-7}$ M) as well as the observed protonation, suggests a similarly important role for the adenine moiety in binding. Indeed, the 6-NH_2 site is altered in ε-EHNA. Thus, in ε-EHNA the observed protonation suggests proper orientation relative to the proton donating group at the active site. By analogy, EHNA may thus undergo a similar protonation, yet the nonyl chain may distort this molecule enough to prevent its deamination, resulting in inhibition.

An extension of the measurement to enzyme bound ε-adenosine (the etheno modification of natural substrate, adenosine) has failed. Although ε-adenosine has an intact ribose moiety, its affinity to ADase is low ($K_1 = 2.2 \times 10^{-5}$ M). Therefore, the concentration of ADase required for equilibrium [6] brings about an inner filter effect. [7] Thus, the above alluded to protonation equilibrium required the use of ε-EHNA.

The peculiar proton sensitivity of an etheno analogue might be proposed for probing the protonation equilibrium in an enzyme active site by means of the relatively sensitive steady-state fluorescence excitation spectroscopy. Since etheno–adenines are probes of energy transduction and molecular genetics, the present approach may be tried there too.

References

[1] R.M. Berne, T.W. Rall, R. Rubio, Developments in pharmacology, In: R.M. Berne, T.W. Rall, R. Rubio (Eds.), Regulatory Function of Adenosine, 2, Martinus Nijhoff Publishers, The Hague, (1983) pp. 142–149.
[2] A.L. Akeson, D.A. Wiginton, J.J. Hutton, J. Cell. Biochem. 39 (1989) 217.
[3] P.P. Trotta, M.E. Balis, Biochemistry 17 (1978) 270.

[5] Or destabilize the neutral form. In either case $\Delta pK_a \sim 2$ is observed, corresponding to 3 Kcal/mole.

[6] The equilibrium binding conditions are achieved when the initial concentration of the enzyme is of the same order of magnitude as the dissociation constant of the ligand–enzyme complex, which is in this case $\sim 10^{-5}$ M. [A.J. Pesce, C.G. Rosen T.L. Pasby (Eds.), Fluorescence Spectroscopy, Marcel Dekker, New York (1981)].

[7] The absorbance of the solution in the given range of wavelengths must be less than 0.2 [F. Schroeder, Methods for Studying Membrane Fluidity, In: Alan R. Liss (Ed.), 1988, pp. 193–217].

[4] D.W. Martin Jr., E.W. Gelfand, Ann. Rev. Biochem. 50 (1981) 845.
[5] N.M. Kredich, M.S. Hershfield, The Metabolic Basis of Inberited Disease, In: C.R. Scrivner et al. (Eds.), McGraw-Hill, New York, (1990) pp. 1045–1075.
[6] M.S. Coleman, J.J. Hutton, Exp. Cell. Res. 94 (1975) 440.
[7] W.P. Schrader, A.R. Stacy, B. Pollara, J. Biol. Chem. 251 (1976) 4026.
[8] M.E. Balis, Ann. N.Y. Acad. Sci. 451 (1985) 142.
[9] N. Porat, D. Gill, A.H. Parola, J. Biol. Chem. 263 (1988) 14608.
[10] I. Durak, R. Cetin, O. Canbolat, D. Cetin, Z. Yurtaslani, A. Unal, Cancer Lett. 84 (1994) 199.
[11] M. Walia, M. Mahajan, K. Singh, J. Med. Res. 101 (1995) 247.
[12] N.O. Kaplan, Methods in Enzymology, In: S.P. Colowick, N.O. Kaplan (Eds.), 2 (1955) 473–478.
[13] M.l. Weisman, V.R. Caiolfa, A.H. Parola, J. Biol. Chem. 263 (1988) 5266.
[14] A.J. Sharff, D.K. Wilson, Z. Chang, F.A. Quiocho, J. Mol. Biol. 226 (1992) 917.
[15] V. Sideraki, K.A. Mohamedali, D.K. Wilson, Z. Chang, R.E. Kellens, F.A. Quicho, F.B. Rudolph, Biochemistry 35 (1996) 7862.
[16] W.P. Schrader, C.A. West, J. Histochem. Cytochem. 33 (1985) 508.
[17] P.P. Trotta, Biochemistry 21 (1982) 4013.
[18] A.H. Parola, N. Porat, V.R. Caiolfa, D. Gill, L.A. Kiesow, M. Weisman, S. Nemschitz, D. Yaron, K. Singer, E. Solomon, Time resolved laser spectroscopy in biochemistry, progress in SPIE, Int. Soc. Opt. Eng. 1204 (1990) 830–842.
[19] R.J. Andy, R. Kornfeld, J. Biol. Chem. 257 (1983) 7922.
[20] G. Skorka, P. Shuker, D. Gill, J. Zabicky, A.H. Parola, Biochemistry 20 (1981) 3103.
[21] J.R. Lakowicz, G. Laczko, H. Cherek, E. Gratton, M. Limkeman, Biophys. J. 46 (1984) 463.
[22] H. Schaeffer, J.C.F. Schwender, J. Med. Chem. 17 (1974) 6.
[23] G.C. Harriman, A.F. Poirot, E. Abushanab, R.M. Midgett, J.D. Stoeckler, J. Med. Chem. 35 (1992) 4180.
[24] J.A. Secrist III, J.R. Barrio, N.J. Leonard, G. Weber, Biochemistry 11 (1972) 3499.
[25] N.J. Leonard, Crit. Rev. Biochem. 15 (1984) 125.
[26] R.A. Agbaria, A.H. Parola, D. Gill, J. Phys. Chem. 98 (1994) 280.
[27] V.R. Caiolfa, D. Gill, A.H. Parola, FEBS Lett. 260 (1990) 19.
[28] C. Frieden, L.C. Kurz, H.R. Gilbert, Biochemistry 19 (1980) 5303.
[29] L.C. Kurtz, C. Frieden, Biochemistry 26 (1987) 8450.
[30] G. Sorolla, European Patent App. 9154 (CL.CO7D473/30), pp. 25–34.
[31] E.K. Keeler, P. Campbell, Biochem. Biophys. Res. Commun. 72 (1976) 575.
[32] H. Wombacher, M. Reuter-Smerdka, Z. Naturforsch. 31c (1976) 18.
[33] J.E. Roberts, Y. Aizono, M. Sonenberg, N.J. Swilslocki, Bioorg. Chem. 4 (1975) 181.
[34] J.J. Sedmak, S.E. Grossberg, Anal. Biochem. 79 (1977) 544.
[35] A.H. Parola, V.R. Caiolfa, I. Bar, S. Rosenwaks, Anal. Biochem. 181 (1989) 383.
[36] W.W. Mantulin, G. Weber, J. Chem. Phys. 66 (1977) 4092.
[37] R.D. Spencer, G. Weber, Ann. N.Y. Acad. Sci. 158 (1969) 361.
[38] I. Natan, G. Fleischer, A. Livne, A. Dvilansky, A.H. Parola, J. Biol. Chem. 254 (1979) 9822.
[39] S. Hazan, I. Fishov, M. Zamai, V.R. Caiolfa, A.H. Parola, Peptides 60 (1995) 333.
[40] A. Alfahel, A. Korngreen, A.H. Parola, Z. Priel, Biophys. J. 70 (1996) 1045.
[41] J.R. Lakowicz, F.G. Prendergast, D. Hogen, Biochemistry 18 (1979) 508.
[42] K.H. Scheller, H. Sigal, J. Am. Chem. Soc. 105 (1983) 3005.
[43] D. Spencer, G. Weber, G.l. Tolman, J.R. Barrio, N.J. Leonard, Eur. J. Biochem. 45 (1974) 425.
[44] R.P. Agarwal, R.E. Parks Jr., J. Methods Enzymol., P.A. Hoffee, M.E. Jones (Eds.), Academic Press, New York, 51 (1978) 502–507.
[45] W.J. Van Blitterswijk, R.P. Van Hoeven, B.W. Van Der Meer, Biochem. Biophys. Acta 644 (1981) 323.
[46] P.M. Weiss, P.F. Cook, J.D. Hermes, W.W. Cleland, Biochemistry 26 (1987) 7378.
[47] N.J. Leonard, Acc. Chem. Res. 15 (1982) 128.
[48] A. Warshel, Biochemistry 20 (1981) 3167.
[49] D.K. Wilson, F.B. Rudolph, Quiocho F.A., Science 252 (1991) 613.
[50] D. Bhaumik, J. Medin, K. Gathy, M.S. Coleman, J. Biol. Chem. 268 (1993) 5464.